WITNESSING THE KEY EARLY PHASE OF QUASAR EVOLUTION: AN OBSCURED ACTIVE GALACTIC NUCLEUS PAIR IN THE INTERACTING GALAXY IRAS 20210+1121

Enrico Piconcelli[1], Cristian Vignali[2], Stefano Bianchi[3], Smita Mathur[4], Fabrizio Fiore[1], Matteo Guainazzi[5], Giorgio Lanzuisi[6], Roberto Maiolino[1], and Fabrizio Nicastro[1,7,8]

[1] Osservatorio Astronomico di Roma (INAF), Via Frascati 33, I-00040 Monte Porzio Catone (Roma), Italy; enrico.piconcelli@oa-roma.inaf.it
[2] Dipartimento di Astronomia, Università di Bologna, Via Ranzani 1, I-40127 Bologna, Italy
[3] Dipartimento di Fisica, Università degli Studi Roma Tre, via della Vasca Navale 84, I-00146 Roma, Italy
[4] Ohio State University, 140 West 18th Avenue, Columbus, OH 43210, USA
[5] European Space Astronomy Centre of the European Space Agency, P.O. Box 78, Villanueva de la Cañada, E-28691 Madrid, Spain
[6] IASF (INAF), via del Fosso del Cavaliere 100, I-00133 Roma, Italy
[7] Harvard-Smithsonian Center for Astrophysics, 60 Garden Street, MS-04, Cambridge, MA 02155, USA
[8] IESL, Foundation for Research and Technology, 711 10, Heraklion, Crete, Greece

ABSTRACT

We report the discovery of an active galactic nucleus (AGN) pair in the interacting galaxy system IRAS 20210+1121 at $z = 0.056$. An *XMM-Newton* observation reveals the presence of an obscured ($N_H \sim 5 \times 10^{23}$ cm^{-2}), Seyfert-like ($L_{2-10\,keV} = 4.7 \times 10^{42}$ erg s^{-1}) nucleus in the northern galaxy, which lacks unambiguous optical AGN signatures. Our spectral analysis also provides strong evidence that the IR-luminous southern galaxy hosts a Type 2 quasar embedded in a bright starburst emission. In particular, the X-ray primary continuum from the nucleus appears totally depressed in the *XMM-Newton* band as expected in the case of a Compton-thick absorber, and only the emission produced by Compton scattering ("reflection") of the continuum from circumnuclear matter is seen. As such, IRAS 20210+1121 seems to provide an excellent opportunity to witness a key, early phase in the quasar evolution predicted by the theoretical models of quasar activation by galaxy collisions.

Key words: galaxies: active – galaxies: interactions – galaxies: nuclei – X-rays: individual (IRAS 20210+1121)

Online-only material: color figures

1. INTRODUCTION

Current supermassive black hole (SMBH) formation and SMBH/galaxy co-evolution models predict an early dust-enshrouded phase associated with rapid SMBH growth triggered by multiple galaxy encounters (Silk & Rees 1998; Di Matteo et al. 2005; Hopkins et al. 2008). Tidal interactions favor both violent star formation as well as funneling of a large amount of gas into the nuclear region to feed (and obscure) the accreting SMBH (e.g., Urrutia et al. 2008; Schawinski et al. 2010). The importance of mergers increases with redshift (Conselice et al. 2003; Lin et al. 2008), and their fundamental role at the peak epoch of luminous active galactic nucleus (AGN, i.e., quasar) and intensive star formation activity at $1.5 \lesssim z \lesssim 3$ is widely accepted.

Over the last few years, an increasing number of interacting and disturbed molecular gas-rich galaxy systems showing both coeval powerful starburst (SB) and quasar activity at high z have indeed been unveiled (e.g., Carilli et al. 2002; Dasyra et al. 2008). The counterparts in the local universe to such luminous, high-z mergers are the (ultra)-luminous infrared ($L_{IR} > 10^{11}\,L_\odot$) galaxies, i.e., (U)LIRGs (Sanders & Mirabel 1996). In particular, these powerful objects should provide the opportunity for probing an inevitable outcome of the hierarchical merging process, i.e., the existence of dust-enshrouded double/multiple SMBHs within the envelope of the host galaxy merger (Colpi et al. 2008). Despite being widely pursued, direct observational evidence for AGN pairs in ULIRGs (as well as in all of the other types of galaxies) has been very limited so far. In the last few years X-ray observations with arcsec angular resolution have provided one of the most efficient tools to disclose such systems. Komossa et al. (2003) discovered the first and unambiguous example of an active SMBH pair separated by

$d \sim 1.4$ kpc in the center of the ULIRG NGC 6240. Additional examples of dual AGNs with a close separation were unveiled by Bianchi et al. (2008) and Ballo et al. (2004) in the ULIRGs Mrk 463 ($d \sim 3.8$ kpc) and Arp 299 ($d \sim 4.6$ kpc), respectively, on the basis of *Chandra* data. Guainazzi et al. (2005b) have reported the discovery of an X-ray bright AGN pair in ESO590-IG066, an early-phase ($d \sim 10.5$ kpc) merging system at $z = 0.03$. It is worth noting that in all these cases hard (>2 keV) X-ray data have been crucial to detect activity from both SMBHs of the galaxy pair. Indeed, at least one pair member lacks optical/IR signatures of AGN activity that suggests we are observing a non-standard AGN phase.

Furthermore, a handful of kiloparsec-scale dual AGN candidates have been recently uncovered in galaxy mergers by the detection of spatially resolved, double-peaked emission line profiles with velocity offsets of a few hundreds km s^{-1} (Civano et al. 2010; Liu et al. 2010), thus doubling the total number of bona fide active SMBH pairs collected so far and, in turn, opening interesting perspectives for further advances in this field of research.

Here, we present the discovery of an AGN pair consisting of a Compton-thick (CT) Type 2 quasar and a heavily obscured Seyfert 2 like source in the interacting galaxy IRAS 20210+1121 (e.g., Section 2). This discovery is based on the imaging and spectral analysis of *XMM–Newton* data described in Section 3. We discuss our results and conclude in Section 4. A cosmology with $H_0 = 70$ km s^{-1} Mpc^{-1}, $\Omega_\Lambda = 0.73$, and $\Omega_M = 0.27$ is assumed throughout (Spergel et al. 2007).

2. IRAS 20210+1121

IRAS 20210+1121 is an interacting system of two galaxies separated by 12.2 arcsec (Arribas et al. 2004; Davies et al.

2002). The larger component of the system, i.e., the southern galaxy (I20210S hereafter), shows a noticeable spiral arm structure, while the northern object (I20210N hereafter) is more spheroidal in shape. Furthermore, a bridge of emission connecting both galaxies is also visible in the optical band. However, narrow-band Hα imaging shows that I20210S has a centrally concentrated, featureless morphology, while I20210N is barely visible (Heisler & Vader 1995). I20210S is a LIRG ($L_{IR} = 7.8 \times 10^{11} L_\odot$) with a Seyfert 2 nucleus at $z = 0.056$ and a [O III] luminosity $L_{[O\,III]} = 2.04 \times 10^{43}$ erg s^{-1} (e.g., Perez et al. 1990; Shu et al. 2007). I20210N has a very faint emission line spectrum, but sufficient to derive the same z of the companion. An important feature of the optical spectrum of I20210N is an intensity ratio [N II] $\lambda 6584$/Hα ≈ 3. Such a value is typical of both LINERs and Seyfert galaxies, and no firm conclusion on the presence of an AGN in this source can be drawn on the basis of these low signal-to-noise ratio data. Furthermore, a near-IR spectroscopic study of I20210N found a featureless near-IR continuum (Burston et al. 2001).

I20210S was detected by *BeppoSAX* at a 2–10 keV flux level of $F_{2-10} \approx 2.9 \times 10^{-13}$ erg cm^{-2} s^{-1} and only ∼160 counts were collected in the 0.1–10 keV band (given the arcmin angular resolution of *BeppoSAX*, any possible emission from I20210N cannot be discerned). The analysis of these data by Ueno et al. (2000) revealed a very flat continuum slope $\Gamma = 0.5^{+0.7}_{-1.0}$ and the remarkable presence of a strong (EW$_{Fe} = 1.6^{+2.3}_{-1.1}$ keV) Fe Kα line that led these authors to suggest that I20210S may host a CT AGN. The observed F_{2-10} to [O III] flux ratio of <0.1 inferred for I20210S also hints for a CT absorber scenario (Guainazzi et al. 2005a). However, it is worth bearing in mind the large errors affecting the spectral parameters derived from this observation.

3. OBSERVATIONS AND DATA REDUCTION

We observed IRAS 20210+1121 with *XMM–Newton* on 2009 May 22 for about 75 ks (ObsID: 0600690101). The observation was performed with the *EPIC* PN and MOS cameras operating in Full-Window mode and with the MEDIUM filter applied. Data were reduced with SAS v9.0 using standard procedures and the most updated calibration files. The event lists were filtered to ignore periods of high background flaring according to the method presented in Piconcelli et al. (2004) based on the cumulative distribution function of background light curve count rates and the maximization of the signal-to-noise ratio. The PN source counts were extracted from a circular region of 10 (I20210N) and 8 (I20210S) arcsec centered at ($\alpha_{2000} = 20^h23^m25^s.04$; $\delta_{2000} = +11°31'47''.7$) and ($\alpha_{2000} = 20^h23^m25^s.35$; $\delta_{2000} = +11°31'30''$), in order to avoid any cross-contamination between the two regions and include the maximum number of counts with $E > 5$ keV. For the two MOS cameras the extraction radius was of 9 arcsec for both sources. The background spectra were extracted from source-free, much larger circular regions on the same chip and close to the target. After this screening, the final net exposure times in the case of I20210S(I20210N) were 61.2(60.1) and 69.7(70) ks for PN and MOS, respectively. Appropriate response and ancillary files for all the *EPIC* cameras were created using RMFGEN and ARFGEN tasks in the SAS, respectively. Spectra were rebinned so that each energy bin contains at least 20 counts to allow us to use the χ^2 minimization technique in spectral fitting.

In this Letter, we present and discuss the PN spectral results only, since this detector has a better sensitivity over the broad
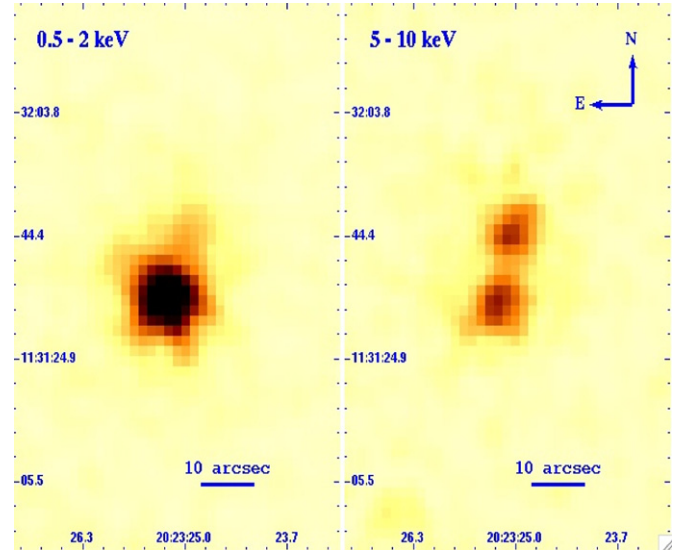

Figure 1. *XMM–Newton EPIC* PN Gaussian-smoothed ($\sigma = 2$ arcsec) image of the interacting galaxy system IRAS 20210+1121 in the 0.5–2 keV (left panel) and 5–10 keV (right panel) energy range.

(A color version of this figure is available in the online journal.)

0.3–10 keV range compared to both MOS cameras (even if co-added together), and above 5 keV in particular. Nonetheless, we checked that consistent results were obtained including the MOS data in our analysis.

4. RESULTS

An important result from the *XMM–Newton* observation is presented in Figure 1, showing the X-ray images of IRAS 20210+1121 in the 0.5–2 and 5–10 keV bands. In the soft band, only the X-ray emission centered on the [O III]-luminous galaxy of the pair, i.e., I20210S, is clearly visible. Whereas the very hard X-ray image reveals the presence of two sources being almost comparable in intensity, and spatially coincident with the radio nucleus of the southern galaxy, or with the optical centroid of the northern galaxy (once an absolute astrometry uncertainty of 2 arcsec and the dispersion of photons due to the point-spread function are considered[9]), respectively. At their redshift, the projected separation between the intensity peaks of both sources in the 5–10 keV image shown in Figure 1 is $d \approx 11$ kpc. The simplest interpretation of the hard X-ray image is that I20210N may also host an obscured AGN, thus revealing, in turn, the presence of an AGN pair in this interacting system. Direct evidence to support this buried AGN pair hypothesis comes from the X-ray spectroscopy of I20210N.

The spectral analysis of *EPIC* data of both sources was carried out using the XSPEC v12 software package. The Galactic column density of $N_H^{Gal} = 9.73 \times 10^{20}$ cm^{-2} derived from Dickey & Lockman (1990) was adopted in all the fits. Henceforth, errors correspond to the 90% confidence level for one interesting parameter, i.e., $\Delta\chi^2 = 2.71$.

We yielded a very good description of the spectrum of I20210N with a typical Compton-thin Seyfert 2 model (e.g., Turner et al. 1997), as shown in Figure 2 (top panel). The primary X-ray continuum power law is absorbed by a column density of $N_H = (4.7^{+1.7}_{-1.0}) \times 10^{23}$ cm^{-2} and exhibits a slope of $\Gamma = 2.0 \pm 0.2$. The emission in the soft portion of the spectrum (the

---

[9] See http://xmm2.esac.esa.int/docs/documents/CAL-TN-0018.pdf for more detail.
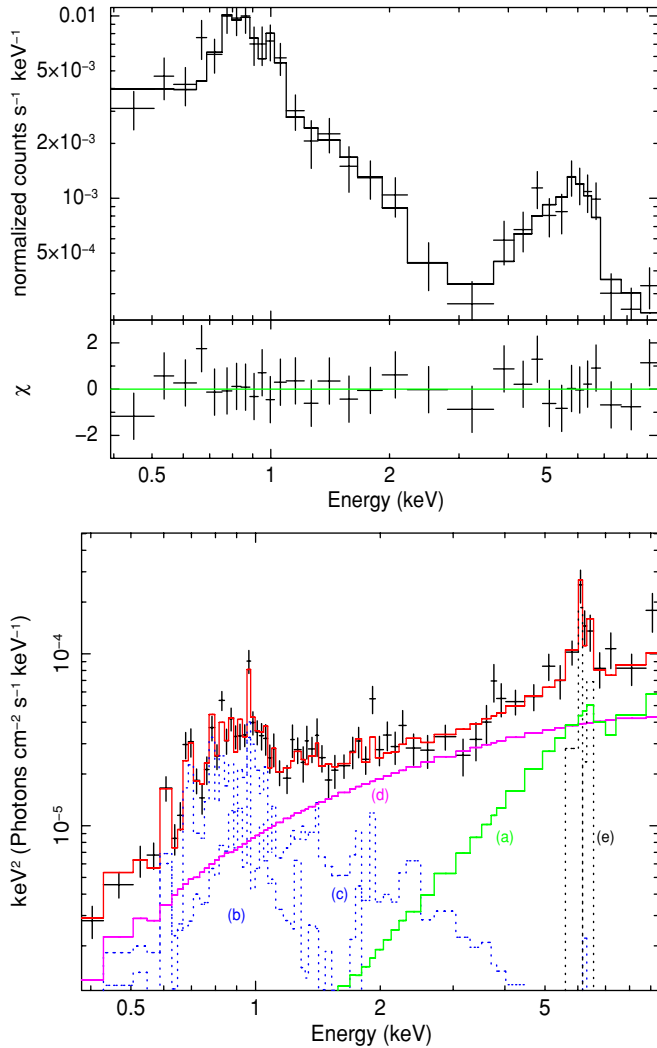
Figure 2. Top: best-fit data and folded model (thick line), plus residuals, of the PN spectrum of I20210N. Bottom: the PN spectrum of I20210S with the "composite" CT AGN+SB best-fit model plotted as a thick line. The individual model components are also shown: (a) pure reflection continuum resulting from a power-law illumination of cold material; (b) and (c) thermal plasma components; (d) cutoff power law associated with the X-ray binaries; and (e) two narrow Gaussian lines at 6.4 and 6.7 keV, respectively. See the text for details.

(A color version of this figure is available in the online journal.)

so-called soft excess component) is well fitted by an additional unabsorbed power law fixing its photon index to that of the absorbed power law, but with a different normalization ($\sim$3% of the primary continuum), plus three narrow Gaussian emission lines. The best-fit values for the energy of these lines are $\sim$0.82, $\sim$0.92, and $\sim$1.07 keV, which can be identified with Fe XVII 3d–2p, Ne IX Kα, and Ne X Kα/Fe XXI 3d–2p transitions, respectively. Such a soft excess component has been detected in most of the obscured AGNs, and it is typically explained as emission from large-scale ($\sim$0.1–1 kpc; see Bianchi et al. 2006) photoionized gas, dominated by a wealth of strong emission lines from hydrogen- and helium-like ions of the most abundant metals, from carbon to sulfur (Guainazzi & Bianchi 2007; Kinkhabwala et al. 2002). Assuming this spectral model (χ^2/dof = 15/20), we measured a 0.5–2 keV flux of 1.6×10^{-14} erg cm^{-2} s^{-1}and a 2–10 keV flux of 1.2×10^{-13} erg cm^{-2} s^{-1}. After correcting for absorption, this flux corresponds to a luminosity of $L_{2-10\,\text{keV}} = 4.7 \times 10^{42}$ erg s^{-1} in

the hard band. Such a value of the 2–10 keV luminosity falls well within the AGN luminosity range (e.g., Maiolino et al. 2003), and thus providing unambiguous evidence for the existence of an active SMBH at the center of I20210N.

The *XMM–Newton* spectrum of I20210S is very complex as shown in Figure 2 (bottom panel). This was expected on the basis of millimeter/IR/optical data that have revealed the simultaneous presence of star-forming and nuclear activity in this galaxy (Horellou et al. 1995; Burston et al. 2001; Perez et al. 1990). In particular, from the 1.4 GHz radio(far-IR) luminosity of I20210S, a star formation rate (SFR) $\sim$ 120(75) $M_\odot$ yr^{-1} can be estimated according to the relationship reported in Ranalli et al. (2003). We have indeed found an excellent description of the *XMM–Newton* data assuming a composite SB+AGN emission model (χ^2_ν/dof = 0.96(65)). The soft X-ray SB emission has been fitted by the superposition of two thermal emission components (MEKAL model in XSPEC) with solar metallicity and a temperature $kT = 0.58 \pm 0.08$ and $kT = 1.25^{+0.31}_{-0.16}$ keV, respectively, in agreement with typical values of temperature measured in other well-known star-forming galaxies (Ptak et al. 1999). The hard X-ray emission has been described assuming an absorbed cutoff-power-law model in the form $E^{-\Gamma} \exp^{-h\nu/kT}$ with photon index $\Gamma = 1.1 \pm 0.2$ and cutoff energy fixed to 10 keV. Such a spectral shape is expected in the case of a contribution from flat-spectrum bright low-mass X-ray binaries and, mostly, from high-mass X-ray binaries (HMXBs), as pointed out by Persic & Raphaeli (2002). Another striking characteristic of the emission from HMXBs is a strong Fe XXV emission line at 6.7 keV, that is indeed observed in the spectrum (see Figure 2, bottom panel) with a poorly constrained value of equivalent width, EW $\sim$ 500 eV. We derived a soft(hard) X-ray luminosity of $L_{0.5-2\,\text{keV}} = 5.2(6.6) \times 10^{41}$ erg s^{-1} for the SB emission. According to Ranalli et al. (2003), these values imply an SFR $\sim$ 110–130 $M_\odot$ yr^{-1}, which is consistent with the SFR values derived both from the radio and far-IR luminosity reported above. The goodness of this match therefore lends further support to the idea that the hard X-ray power-law component originates from the population of HMXBs expected to be present in the SB regions of I20210S.

Our best-fit model to the *XMM–Newton* data includes a component due to X-ray reflection from cold circumnuclear matter with $N_H \gtrsim 1.6 \times 10^{24}$ cm^{-2} (i.e., CT) and an Fe Kα emission line to account for the reprocessed AGN emission visible in the 0.3–10 keV band, the X-ray primary continuum emission being completely blocked in this energy range (Ghisellini et al. 1994).

The energy centroid of the line is at $6.35^{+0.06}_{-0.04}$ keV and the EW measured with respect to the reflection continuum is 900 ± 400 eV. These values unambiguously indicate an origin from reflection in cold circumnuclear CT material. The X-ray primary continuum from the AGN is totally depressed in the *EPIC* band, as expected in the case of a CT absorber. We derive an AGN flux ($F_{2-10} = 7.7 \times 10^{-14}$ erg cm^{-2} s^{-1}), accounting for $\sim$47% of the total (AGN + SB) 2–10 keV flux. The observed $L_{2-10\,\text{keV}}$ of the AGN component is 5.3×10^{41} erg s^{-1}: according to the reflection-dominated/CT scenario it should be at most 1%–2% of the de-absorbed luminosity (e.g., Comastri 2004; Levenson et al. 2006), suggesting an intrinsic $L_{2-10\,\text{keV}} > (0.5-1) \times 10^{44}$ erg s^{-1}, which is consistent with the expectation based on the $L_{[O\,\text{III}]}$. This result matches well with the hypothesis of a CT absorbing screen and, hence, the presence of a quasar 2 (with $L_X > 10^{44}$ erg s^{-1}) at the heart of I20210S.

We also tried a model assuming a transmission scenario for the AGN emission below 10 keV. We fixed the photon index of

the continuum power law to the canonical value of $\Gamma = 1.8$ due to the limited statistics. This fit is statistically as good as the reflection-dominated fit discussed above, with a resulting $N_H = (3.2^{+2.0}_{-1.5}) \times 10^{23}$ cm^{-2}. However, this N_H implies an $L_{2-10\,\mathrm{keV}} = 1.2 \times 10^{42}$ erg s^{-1}, which is 2 orders of magnitude lower than expected on the basis of the $L_{[\mathrm{O\,III}]}$, and an EW of the Fe Kα line against the absorbed continuum of $\sim$250 eV (Ghisellini et al. 1994; Guainazzi et al. 2005a), while we measured an EW = 620 ± 260 eV. These two considerations tend to disfavor the transmission scenario and lead us to assume the presence of a CT screen along our line of sight to the nucleus of I20210S as the most likely interpretation of the *XMM–Newton* data.

5. CONCLUSIONS

The *XMM–Newton* observation of IRAS 20210+1121 presented here has unveiled the existence of an obscured AGN pair placed at a projected distance of $d \sim 11$ kpc in this interacting galaxy system. In particular, we have discovered a Seyfert 2 like AGN in the nucleus of I20210N, for which neither optical nor near-IR spectroscopic observations have provided unambiguous evidence for the existence of an active SMBH at its center. Furthermore, the results of our spectral analysis have provided evidence that the southern member of the pair, the LIRG I20210S, optically classified as a Seyfert 2 galaxy, likely hosts a powerful AGN hidden behind a CT absorber. The AGN is embedded in a strong SB emission accounting for $\sim$50% of the 2.0–10 keV flux measured for I20210S.

IRAS 20210+1121 is therefore a rarely observed example of CT quasar 2 plus optically "elusive" AGN pair observed during the initial stage of the interaction between their host galaxies, that are still easily identifiable, but also show a well-developed tidal bridge (Arribas et al. 2004). As such, this system seems to provide an excellent opportunity to witness a merger-driven phase of quasar fueling predicted by most of the evolutionary models based on the co-evolution of SMBHs and their host galaxies.

The mismatch between the optical/near-IR and the hard X-ray appearances of the nuclear spectrum of I20210N can be explained in terms of a completely blocked line of sight to the nuclear region, so that the narrow line region (NLR) is also obscured (Maiolino et al. 2003). The geometrical properties of the absorber should be thereby different from those assumed in typical Seyfert 2 galaxies, i.e., a parsec-scale torus-like shape. The absorber in I20210N may be characterized by a much more extended distribution (over a few hundreds of pc) in a way that obscures the NLR. Alternatively, it could be spherically symmetric blocking the flux of ionizing UV photons responsible for the line emission in the NLR. The AGN in I20210N is revealed through hard X-ray observations only; this feature is shared by most AGN pairs discovered lately thanks to hard X-ray observations (e.g., Komossa et al. 2003; Guainazzi et al. 2005b; Bianchi et al. 2008). An intriguing explanation for this behavior can be given in terms of a dust-enshrouded circumnuclear environment due to merger-induced processes favoring gas concentration in the galaxy center. For instance, there may be an extra-torus optical/X-ray absorber lying far from the nucleus, and outside the NLR, being likely associated with prominent dust lanes in the disturbed host galaxy.

The discovery of a CT quasar 2 in I20210S is in itself very important given the paucity of low-z members of this peculiar class of AGN detected so far, which are considered a key ingredient in the synthesis models of the cosmic X-ray

background. This can be ascribed to their low surface density and their absorption-induced faintness at the wavelengths where classical large-area surveys have been performed (i.e., optical, near-IR, UV, and X-rays), that make the luminous CT AGN population extremely difficult to observe. Selection criteria based on mid-IR versus optical colors (e.g., Lanzuisi et al. 2009, and references therein) have been proven to be efficient in discovering a large number of heavily obscured quasar candidates at $z \geqslant 1$. Unfortunately, most of these sources are detected at very faint flux levels ($F_{2-10} \ll 10^{-14}$ erg cm^{-2} s^{-1}), making an appropriate X-ray spectral follow-up extremely time consuming.

Further support to the CT quasar 2 nature for the AGN in I20210S is provided by the comparison of the expected value of the X-ray bolometric correction $r_{X,\mathrm{bol}} \equiv L_{2-10\,\mathrm{keV}}/L_{\mathrm{bol}} = 0.043 \times (L_{\mathrm{bol}}/10^{45})^{-0.357}$ (assuming a bolometric luminosity of $L_{\mathrm{bol}}(\approx L_{\mathrm{IR}}) \approx 3 \times 10^{45}$ erg s^{-1}) for a typical quasar from Piconcelli et al. (2007), and the values of $r_{X,\mathrm{bol}}$ calculated using the hard X-ray luminosity inferred for the CT and transmission scenario, respectively. In fact, the expected value of $r_{X,\mathrm{bol}} = 0.03$ is consistent with that derived assuming a $L_{2-10\,\mathrm{keV}} > 5 \times 10^{43}$ erg s^{-1} (estimated from the $L_{[\mathrm{O\,III}]}$ luminosity and a CT absorber), i.e., $r_{X,\mathrm{bol}} > 0.02$, but it is much higher than $r_{X,\mathrm{bol}} = 0.0004$ derived for a $L_{2-10\,\mathrm{keV}} = 1.2 \times 10^{42}$ erg s^{-1}.

Detection of objects such as I20210S is important because they provide useful templates to explore the multi-wavelength properties of the obscured accretion phenomenon without any luminosity bias. The observed properties of I20210S can be interpreted in the framework of an evolutionary merger-driven scenario according to which a peculiar dust-cocooned, early stage in the life cycle of quasars is linked to a period of intense star-forming activity in the interacting host galaxy (Silk & Rees 1998; Treister et al. 2010). An easily observable outcome of this scenario is indeed an enhancement of the IR luminosity, with the system undergoing a (U)LIRG phase powered both by the SB and the AGN. Furthermore, Horellou et al. (1995) measured a molecular hydrogen mass $M_{\mathrm{H_2}}$ of $4.1 \times 10^9 \, M_\odot$ for I20210S that implies an $L_{\mathrm{FIR}}/M_{\mathrm{H_2}}$ ratio $\geqslant 100 \, L_\odot \, M_\odot^{-1}$, i.e., a value typical for gas-rich mergers (Sanders et al. 1991). According to model predictions, the SMBH at the center of I20210S should be accreting close to the Eddington rate, in agreement with the quasar-like values of $L_{[\mathrm{O\,III}]}(L_{2-10\,\mathrm{keV}})$ measured(estimated) for the AGN.

The interacting system IRAS 20210+1121, therefore, surely deserves deeper investigations in the future in order to examine the possible presence of any structures associated with the merging process (i.e., outflows, inflows, and obscured SB regions) which could not be revealed by the observational data available so far, but potentially very useful for our understanding of quasar evolution and AGN/SB triggering mechanisms.

REFERENCES

Arribas, S., Bushouse, H., Lucas, R. A., Colina, L., & Borne, K. D. 2004, AJ, 127, 2522
Ballo, L., Braito, V., Della Ceca, R., Maraschi, L., Tavecchio, F., & Dadina, M. 2004, ApJ, 600, 634

Bianchi, S., Chiaberge, M., Piconcelli, E., Guainazzi, M., & Matt, G. 2008, MNRAS, 386, 105

Bianchi, S., Guainazzi, M., & Chiaberge, M. 2006, A&A, 448, 499

Burston, A. J., Ward, M. J., & Davies, R. I. 2001, MNRAS, 326, 403

Carilli, C. L., et al. 2002, AJ, 123, 1838

Civano, F., et al. 2010, ApJ, 717, 209

Colpi, M., Dotti, M., Mayer, L., & Kazantzidis, S. 2008, in Proc. Conf. on 2007 STScI Spring Symposium: Black Holes, ed. M. Livio & A. M. Koekemoer (Cambridge: Cambridge Univ. Press), arXiv:0710.5207

Comastri, A. 2004, in Supermassive Black Holes in the Distant Universe, ed. A. J. Barger (Astrophys. Space Sci. Lib. 308; Dordrecht: Kluwer), 245

Conselice, C. J., Bershady, M. A., Dickinson, M., & Papovich, C. 2003, AJ, 126, 1183

Dasyra, K. M., Yan, L., Helou, G., Surace, J., Sajina, A., & Colbert, J. 2008, ApJ, 680, 232

Davies, R. I., Burston, A., & Ward, M. J. 2002, MNRAS, 329, 367

Dickey, J. M., & Lockman, F. J. 1990, ARA&A, 28, 215

Di Matteo, T., Springel, V., & Hernquist, L. 2005, Nature, 433, 604

Ghisellini, G., Haardt, F., & Matt, G. 1994, MNRAS, 267, 743

Guainazzi, M., & Bianchi, S. 2007, MNRAS, 374, 1290

Guainazzi, M., Matt, G., & Perola, G. C. 2005a, A&A, 444, 119

Guainazzi, M., Piconcelli, E., Jimenez-Bailon, E., & Matt, G. 2005b, A&A, 429, L9

Heisler, C. A., & Vader, P. J. 1995, AJ, 110, 87

Hopkins, P. F., Hernquist, L., Cox, T. J., & Keres, D. 2008, ApJS, 175, 356

Horellou, C., Casoli, F., Combes, F., & Dupraz, C. 1995, A&A, 298, 743

Kinkhabwala, A., et al. 2002, ApJ, 575, 732

Komossa, S., Burwitz, V., Hasinger, G., Predehl, P., Kaastra, J. S., & Ikebe, Y. 2003, ApJ, 582, L15

Lanzuisi, G., Piconcelli, E., Fiore, F., Feruglio, C., Vignali, C., Salvato, M., & Gruppioni, C. 2009, A&A, 498, 67

Levenson, N. A., Heckman, T. M., Krolik, J. H., Weaver, K. A., & Zycki, P. T. 2006, ApJ, 648, 111

Lin, L., et al. 2008, ApJ, 681, 232

Liu, X., Greene, J. E., Shen, Y., & Strauss, M. A. 2010, ApJ, 715, L30

Maiolino, R., et al. 2003, MNRAS, 344, L59

Perez, E., Manchado, A., Garcia-Lario, P., & Pottash, R. 1990, A&A, 227, 407

Persic, M., & Rephaeli, Y. 2002, A&A, 382, 843

Piconcelli, E., Fiore, F., Nicastro, F., Mathur, S., Brusa, M., Comastri, A., & Puccetti, S. 2007, A&A, 473, 85

Piconcelli, E., Jimenez-Bailon, E., Guainazzi, M., Schartel, N., Rodriguez-Pascual, P. M., & Santos-Lleo, M. 2004, MNRAS, 351, 161

Ptak, A., Serlemitsos, P., Yaqoob, T., & Mushotzky, R. 1999, ApJS, 120, 17

Ranalli, P., Comastri, A., & Setti, G. 2003, A&A, 399, 39

Sanders, D. B., & Mirabel, I. F. 1996, ARA&A, 34, 749

Sanders, D. B., Scoville, N. Z., & Soifer, B. T. 1991, ApJ, 370, 158

Schawinski, K., Dowlin, N., Thomas, D., Urry, C. M., & Edmondson, E. 2010, ApJ, 714, L108

Shu, X. W., Wang, J. X., Jiang, P., Fan, L. L., & Wang, T. G. 2007, ApJ, 657, 167

Silk, J., & Rees, M. J. 1998, A&A, 331, L1

Spergel, D. N., et al. 2007, ApJS, 170, 377

Treister, E., Natarajan, P., Sanders, D., Urry, C. M., Schawinski, K., & Kartaltepe, J. 2010, Science, 328, 600

Turner, T. J., George, I. M., Nandra, K., & Mushotzky, R. F. 1997, ApJS, 113, 23

Ueno, S., Ward, M. J., O'Brien, P. T., Stirpe, G. M., & Matt, G. 2000, Adv. Space Res., 25, 823

Urrutia, T., Lacy, M., & Becker, R. H. 2008, ApJ, 674, 80